Expression and functional comparison of control and 3' deletion human *NRXN1* isoforms in *C. elegans*

Dustin Haskell[1] & Michael P. Hart[1,2]

Affiliations

[1]Department of Genetics, Perelman School of Medicine, University of Pennsylvania

[2]Autism Spectrum Program of Excellence, Perelman School of Medicine

* corresponding author Michael P. Hart – email: hartmic@pennmedicine.upenn.edu

Abstract

Neuropsychiatric conditions including Schizophrenia are historically difficulty to study *in vivo* due to the extensive genetic heterogeneity present between patients. Recent exome sequencing of a Schizophrenia patient cohort identified a set of 3' deletions present within multiple highly expressed α-isoforms of the synaptic adhesion molecule Neurexin1 (*NRXN1*), a gene that is broadly implicated across many neurodevelopmental and neuropsychiatric disorders. To understand how isoform differences and mutations within isoforms impact neuronal function and behaviors, we expressed 8 *NRXN1* isoform variants in *C. elegans* and tested their effects on a stereotyped food-deprivation response and social feeding behavior. Overall, expression of the NRXN1 isoforms followed a pattern similar to that of the endogenous orthologue NRX-1, with expression primarily localized to the nerve ring in the head of the animal. However, several isoform variants displayed distinct localization, with ectopic or abnormal expression in neuronal cell bodies. We observed in the food deprivation response behavior that the isoforms (both control and 3' deletion variants) fell into one of three phenotypic categories; unchanged, partial rescue, or gain of function. A similar trend was observed for social feeding behavior; most of the *NRXN1* isoforms had no impact compared with *npr-1;nrx-1* controls, but some had partial rescue or induced stronger phenotypes. In summary, *NRXN1* isoforms are able to partially rescue behavioral defects caused by the loss of *nrx-1*, suggesting that they may functionally replace the endogenous protein. Further, we identified differential impacts between some control and 3' deletion isoform variants, confirming pathogenic impact of 3' deletion isoforms in behavior. Overall, *C. elegans* presents a genetically tractable model in which to study the impacts of protein coding deletions associated with human neuropsychiatric conditions that impact genes with many isoforms on robust and stereotyped behaviors *in vivo*.

Introduction

The evolution of complex behavioral traits came about through selective pressures across distinct and diverse populations through diversification of neurodevelopmental and neuronal functional traits[1]. Strongly damaging mutations and variants in genes essential and important for neurodevelopment are generally selected against, but less damaging or partially penetrant variants can have a range of phenotypic severity[1,2]. Selective pressures on genes with less severe variants, cam influence non-essential behavioral traits and drive evolutionary changes in behaviors through diversifying development and function of the brain[3]. Some changes in behaviors that result within this evolutionary trajectory can include those associated with neuropsychiatric disorders[4]. However, the complex genetic and neuronal landscape of human neurodevelopment, which includes incredibly diverse neuronal subtypes with unique developmental trajectories, has obscured our understanding of the molecular and neuronal underpinnings of behaviors observed in neuropsychiatric disorders like schizophrenia.

To understand the network of neuronal genes driving neurodevelopment and neuropsychiatric disorders, case control and large gene association studies have identified genes associated with risk for disorders diagnosed by behavioral changes, including schizophrenia [5–8]. Interestingly, there is overlap of some genes (and similar perturbations) implicated across multiple conditions and disorders defined by shared and distinct behavioral changes[9–12]. Which raises many questions, for example, What are the roles of these genes at the neuron and circuit level that make them essential for development of many behaviors? Do different variants within a single gene lead to specific neurodevelopmental trajectories or functional changes that result in behavioral changes associated with different disorders? Overall, to understand how specific changes in a gene and across many genes associated with a disorder can lead to alterations in disparate behaviors will require a mechanistic understanding of how variants alter function of genes, ideally linked to behavioral changes.

To begin to answer some of these questions, one approach is to focus on a subset of associated genes and variants[5,11]. Synaptic adhesion molecules are essential for synaptogenesis, organization, and function by establishing synaptic connectivity and polarity through protein-protein interactions, leading to important behavioral functions[13–15]. Among the best studied synaptic adhesion molecules are neurexins (NRXN). Mammals have three neurexin genes, *NRXN1-3,* from which two separate promoters generate a long α-isoform and a shorter β-

isoform[16–18]. Additionally, *NRXN1* also produces a very short γ-isoform from an overlapping and internal promoter[18]. In contrast to mammals, *Drosophila* and *C. elegans* encode a single neurexin orthologue[19,20], with the *C. elegans* gene *nrx-1* encoding a long α-isoform and short γ-isoform similar to mammalian *NRXN1*[21].

Like many transmembrane synaptic adhesion proteins, neurexins are comprised of a large extracellular domain containing multiple domains for protein-protein interactions as well as short intracellular domain for synaptic scaffolding and signaling[13,22]. Historically, neurexins act primarily with a cognate binding partner neuroligins to establish pre-synaptic and post-synaptic polarity[23,24]. Early work was consistent with both proteins being essential for Ca^{2+}-dependent neurotransmission at both excitatory and inhibitory synapses[25–27]. Later work clarified that neurexins' interactions and roles at the synapse are far more complex, with the protein showing tissue, cell type, and even synapse-type specific mechanisms. Many additional binding partners have been subsequently identified (including neurexophilin, dystoglycan, LRRTM proteins, and cerebellin) which greatly expand the possible mechanisms through which neurexins act[17,28]. From a structural perspective neurexin is relatively simple, with the α-isoform having six LNS domains periodically interspersed with EGF-like domains. However, additional complexity arises from a number of commonly utilized alternative splice sites (five in the α-isoform and 2 in the β-isoform of *NRXN1*), giving the possibility of over 1,000 possible splice variants[29]. However, RNAseq data suggests that only a smaller group of isoforms (~200 alpha isoforms) of the total permutations are expressed in any given tissue or cell type[30–32]. Detailed mechanistic study of these splice sites uncovered several roles for alternative splicing of neurexins in changing binding affinity to specific ligands and partners like neuroligin, and controlling the ratio of neurexin isoforms in a given synapse[33].

Initial characterizations of the three mammalian neurexins suggested similarity in functions and redundancy, however, tissue heterogeneity, developmental differences, and isoform/splice variants have demonstrated a complexity in the functions of each neurexin gene and even isoforms[13]. In contrast, the single neurexin orthologue in *C. elegans* and flies is well conserved and provides a model to study the mechanisms and effects of neurexin. Given that neurexin has many important roles in synaptic development, function, and maintenance, it is not surprising that genetic variation across neurexin genes are associated across many neuropsychiatric disorders and conditions. For example, perturbations ranging from point mutations to large exonic deletions in

NRXN1 have been associated with autism, Tourette's, Bipolar disorder, and Schizophrenia[13]. Recent work has shown copy-number variants (deletions in exons 1-5) of neurexin contribute significantly to the risk of schizophrenia[34]. Furthermore, heterozygous exonic deletions are consistently found in schizophrenia patients, some of which have been implicated in the impairment in neurotransmitter release and neuronal development and an overall reduction in neuronal activity[35]. How different variants in the *NRXN1* gene impact its function to ultimately result in behavioral differences is not well understood, in part due to the complexity of neurexin isoforms, which can be differentially impacted by variants across the gene length. Even deletions in *NRXN1*, which are traditionally thought to introduce loss of function of specific isoforms, were found to result in generation of novel isoforms not generated from the intact locus.

Here we used *C. elegans* to compare the impact of isoforms derived from a patient harboring a 3' *NRNX1* deletion on protein expression and localization, and neuronal function and behavior. We found that control isoforms, generated from the intact allele, and 3' deletion novel isoforms of *NRXN1* are able to induce differential behavioral outputs across several phenotypic assays when comparing both different control isoforms and single control isoform and its corresponding 3' deletion variant isoform. We showed that several control and 3' deletion isoforms are capable of partially rescuing behavioral phenotypes observed with loss of *nrx-1*, suggesting they may be in part function similarly to NRX-1α-isoform. In addition, several isoform variants show gain of function phenotype across multiple behavioral assays indicating they may represent a pathogenic isoform variant.

Methods

Cloning

NRXN1 isoform cDNAs were acquired in lentiviral plasmids from the lab of Kristen Brennand (Yale)[36]. To generate plasmids for expression of human *NRXN1* in *C. elegans*, *NRXN1* cDNAs were cloned into pMPH34 (p*ric-19::sfGFP::nrx-1(α)*)[37] by Epoch Life Sciences, replacing the existing worm *nrx-1*α cDNA. This plasmid drives expression in all neurons using the *ric-19* promoter and a neutral *unc-54* 3' UTR. To remove the N-terminal signal sequence of human *NRXN1*, RF cloning was utilized (all plasmids are listed in Supplemental Table 1). After cloning all plasmid sequences were confirmed via Sanger Sequencing.

Strain Construction and Worm Maintenance

Animals were maintained under normal growth conditions (~20° C) on normal NGM media[38]. Plates were seeded with *E. coli* OP50 to provide food. *NRXN1* isoform transgenic animals were generated by injecting the human *NRXN1 C. elegans* expression plasmids for each *NRXN1* isoform. Standard procedure was used for microinjections. *NRXN1* isoforms were injected at a concentration of 40 ng/μL along with 20 ng/μL of a co-injection marker (either p*lin-44::gfp* or p*unc-122::mScarlet*). Injections were done into the null allele *nrx-1(wy778)*. Once stable extrachromosomal lines were established and characterized for transmission and variability, transgenes were crossed into the *npr*-1*(ad609)* background for the social feeding assays. All strains used are listed in Supplemental Table 1.

Food deprivation behavioral response and activity assays

Animal locomotion and activity levels were analyzed using the WorMotel device as previously described[37,39]. Briefly, each of the 48 wells in the WorMotel chip were filled with standard NGM and allowed to cool. For food deprivation conditions, young adult animals were picked off a plate into a well of M9 media to remove any bacteria from their cuticle. Each animal was then carefully pipetted in 1μL of M9 and placed in a WorMotel well. Once all the animals had been pipetted the liquid was allowed to fully dry before starting the behavioral assay. The WorMotel was placed in a 100 mm petri dish humidified with a wet kimwipe to maintain room level humidity.

The WormWatcher imaging platform was utilized to capture images as previously described[39], with images being captured every 10 seconds for 8 hours. Previously published custom MATLAB code was used to process and analyze the images. The total pixels displaced over a 1 hour period was calculated for each well. Images were manually inspected to remove any wells with escaped, sickly, or stuck animals which were excluded from final analysis. Each was run (3-5) individual replicates, which were combined.

Social feeding behavioral assay

To assay social feeding behavior, 6-well culture plates were filled with NGM media (6mLs) and seeded with 75 μL of *E. coli* OP50 and allowed to dry overnight. To assess levels of social feeding aggregation, 50 L4 animals were picked onto the seeded wells. Excess bacteria

transfer was avoided prevent buildup of the bacterial lawn at later timepoints. To prevent condensation during imaging, a small amount of Tween20 was used to coat the surface of the 6-well lid. The plates are imaged using the WormWatcher automated imaging platform (Tau Scientific) for a total of 20 hours with a cluster of 10 images (over a 1-minute timecourse) being taken every hour. Quantification of social feeding aggregation was performed as previously described[40]. Briefly, a worm is considered aggregating if it is in contact with two or more other worms.

Microscopy

Young adult animals were anesthetized in ~4 μL of 100 μM sodium azide before being immobilized on a standard 5% agarose pad and coverslip. A Leica inverted TCS SP8 laser-scanning confocal microscope with 60x objective lens was used to capture the head regions of each animal to analyze the expression and localization of each *NRXN1* isoform within the nerve ring surrounding the pharynx. Z-stacks were set at 0.5 microns, and Z-imaging captured the full Z-plan of tissue. Consistent laser power and gain settings were used in order to standardize analysis of the expression patterns and levels. Micrographs were generated by generating a SumStack of the available Z-stacks to produce a compressed expression pattern in the nerve ring.

Statistics

The number for each experiment was based on previous studies and effect size, with each experiment performed with at least 3 independent replicates and each trial performed with matched controls[37,40]. All data were analyzed and plotted in GraphPad Prism 10 and statistical significance was determined using one-way ANOVA with Tukey's post-hoc test. For comparisons of two data sets, a two-tailed unpaired t-test was used to compare significance. Error bars on figures represent standard error of the mean (SEM) and p-values are shown in each figure to indicate significance ($P<0.05$).

Results

Human *NRXN1* isoform expression and localization in *C. elegans* neurons

To analyze potential differences across the *NRXN1* isoforms, we compared them to the longest possible α-isoform of *NRXN1*. The deletions were mapped onto the genomic locus and

protein domain architecture, and all 4 of the 3' deletion isoform lack exons 21 and 22 at the C-terminus of the protein **(Figure 1A)**. Furthermore, the deletion is localized to the last extracellular region of the protein before the transmembrane domain, including a portion of the last LNS domain, potentially affecting both localization adjacent to the membrane and the flexibility and interactions involving LNS6. Indeed, removal of exons 21/22 significantly reduces the number of unstructured residues present between the transmembrane domain and the globular domains (**Figure 1B**).

To better understand the functional impact of the deletion on different isoforms, we expressed the human *NRXN1* isoforms in all neurons of *C. elegans*. To make a humanized *NRXN1 C. elegans*, we injected each *NRXN1* isoform cDNA into animals with a large deletion in the single ortholog of neurexin (*nrx-1*) that removes the majority of the alpha and all of the gamma isoform coding regions, and acts as a functional null (*nrx-1(wy778))*. We were able to observe expression of all of the human *NRXN1* isoforms, which had expression patterns (and levels) similar to the same transgenic expression of *nrx-1*[37], with localization to neurons and the nerve ring (**Figure 2A**). Normal expression of endogenous NRX-1 shows a diffuse punctate pattern of expression across the axons of the nerves, sometime extending down towards nerve cord. Typically, there is very little expression in the cell bodies of the head neurons, nor within projections extended towards the nose. In contrast, several of the isoform variants (particularly SS47 and SS73, representing the control and 3' deletion versions of a single isoform, respectively) showed ectopic expression in the cell bodies of one or more head neurons. The SS73 variant in particular showed biased localization of the NRXN1 to the cell bodies of the neurons, with only a faint and diffuse expression patterns appearing in the underlying axonal projects (**Figure 2B**). Lastly, variants such as SS89 showed a distinct mixture of diffuse and punctate expression of NRXN1 in both the cell bodies and axonal projection of the nerve rings that was not observed in the other variants (**Figure 2B**).

NRXN1 isoforms display distinct functions on food-deprived activity levels

We next set out to test the functional impact of each isoform on neuronal and circuit function, using behavioral phenotypes of loss of *nrx-1*. Previous work has shown that *C. elegans* have a robust response to food deprivation, characterized by a significant and sustained increase in their activity levels compared to animals with food[37]. Several gene mutants show behavioral

phenotypes in this behavioral assay, including *nrx-1* mutants, which have a significantly reduced activity upon food deprivation. Transgenic experiments showed that the γ-isoform and the α-isoform of *nrx-1* play distinct temporal roles in the initiation and maintenance, respectively, of hyperactivity upon food deprivation[37].

To test whether the *NRXN1* isoforms could rescue the *nrx-1(wy778)* behavioral phenotype, we utilized the WorMotel assay and assessed activity levels of animals without food. In comparison to control animals (N2), the *nrx-1(wy778)* animals showed a significant decrease in activity, which neuronal expression of NRX-1α was able to partially rescue, as expected (**Figure 3A**). Animals expressing the *NRXN1* isoforms showed differences in the ability to impact activity levels *of nrx-1(wy778)* animals. Two of the four control isoforms (SS71 and SS75) displayed partial rescue the *nrx-1(wy778)* phenotype, suggesting that they may be able to compensate for the loss of NRX-1α (**Figure 3A, left panel**). In comparison, none of the 3' deletion *NRXN1* isoforms displayed any rescue the *nrx-1(wy778)* phenotype, and indeed two of the 3' deletion isoform variants (SS77 and SS89) showed a gain of function phenotype, where their activity was lowered even further than the *nrx-1* null animals (**Figure 3A, right panel**). Overall, the isoforms could be functionally categorized using this behavioral phenotype: unchanged (where the activity levels were similar to *nrx-1(wy778)* (**Figure 3B**)), partial rescue (**Figure 3C**), and gain of function (where activity levels were further reduced (**Figure 3D**)).

NRXN1 isoforms show diverse social feeding behaviors

To further test the impact of the *NRXN1* isoforms, we also analyzed their functional impact on social feeding behavior, specifically the aggregation of *C. elegans* into groups on food. To perform this assay, all transgenic *nrx-1(wy778)* strains were crossed into the *npr-1(ad609)* background, which serves to induce aggregation. Loss of function experiments would suggest that the *npr-1* induced aggregation behavior is strongly modulated by NRX-1 α-isoform and thus represents a assay sensitive to NRXN1 functionality[40]. First, we tested the impact of *NRXN1* isoforms on social feeding behavior in solitary control background (*nrx-1(wy778))* and observed no significant aggregation in control animals or animals expressing the 8 *NRXN1* isoforms variants (4 control isoforms and their 4 corresponding 3' deletion variants) (**Supplemental Figure 1**). However, expression of the *NRXN1* isoforms in the social control *npr-1(ad609)* background we observed a range of impacts on social feeding behavior (**Figure 4A**). The *npr-1(ad609)* social

feeding control has high levels of aggregation (averaging around 40/50 animals), whereas our *nrx-1(wy778); npr1-(ad609)* control has a significantly lower level of aggregating animals **(Figure 4A/B)**. The *NRXN1* control isoforms had variable impact, where 3 did not appear to impact levels of aggregation compared to *nrx-1(wy778); npr1-(ad609)* animals, while SS75 significantly increased aggregation and was able to fully rescue the *nrx-1* phenotype (**Figure 4A, left panel**). Interestingly, 3 of the 3' deletion isoforms significantly increased aggregation of *nrx1(wy778),* with SS73 increasing to a level indistinguishable from *npr-1(ad609)* levels (**Figure 4A, right panel**). Additionally, similar to the food deprivation response, SS89 displayed a strong gain of function phenotype, with aggregation significantly lower than the *nrx-1(wy778); npr1-(ad609)* control (**Figure 4A, right panel**).

Discussion

Synaptic adhesion proteins such as NRXN1 are widely regarded as essential drivers of synaptic assembly and organization as well as maintenance of their overall synaptic function. While small perturbations or partial loss of the neurexin family in mammals is generally tolerated[27], these changes are still implicated in a number of developmental , neuronal, and behavioral changes[13,35,36]. In parallel, with the creation of large genotyping and genome sequencing projects, it has emerged that heterozygous insertions/deletions, point mutations, and copy number variants in NRXN1 contribute to the genes association with various human conditions, indicating that these variants impact protein function[13,17]. When adding in these lines to evidence with the immensely complex Neurexin splicing network a highly intricate picture of neurexin function begins to appear.

In this work, we characterized the impact of expressing four highly expressed *NRXN1* isoforms (both control and 3' deletion variants) isolated from schizophrenia-derived hiPSCs[36]. Leveraging the benefits of a *C. elegans* model, we showed that small isoform differences can significantly alter the effects on two behavioral outputs, starvation-induced activity response and social feeding. Furthermore, we detected behavioral and molecular differences between control and 3' deletion variants of individual isoforms. Overall, the results suggest that at least one isoform generated by 3' deletion in *NRXN1* may have pathogenic roles in neurons, leading to behavioral defects. Given the genetic tractability of the worm neuronal connectome, this work opens the possibility to better understand the distinctive roles and/or mechanisms of individual neurexin

isoforms, a task that is next to impossible in *in vivo* mammalian models. In the long run understanding isoform specific roles and how variation (such as the 3' deletions we modeled) can affect functionality could open new avenues of research leading to more effective treatments or therapies for genetically heterogeneous neuropsychiatric diseases like schizophrenia.

Acknowledgements

The authors thank the labs of John I. Murray, Colin C. Conine, David M. Raizen, and Meera V. Sundaram for their feedback on this project. We also thank members of the Hart lab for comments on the manuscript. Some strains were provided by the CGC, which is funded by NIH Office of Research Infrastructure Programs (P40 OD010440). The authors thank Kristen J. Brennand and Michael B. Fernando for providing plasmids and advice. This work was supported in part by the Autism Spectrum Program of Excellence, a Simons Foundation Bridge to Independence award (MPH), NIH R56MH096881 (MPH), and NIH R35GM146782 (MPH).

Author Contributions

DH and MPH conceived and designed the study and experiments, and DH conducted all experiments, processed, analyzed, and interpreted all data with help from MPH. DH wrote the manuscript with assistance from MPH.

Competing Interests

The authors declare no conflicts of interest.

References

1. McClellan, J. M. *et al.* An evolutionary perspective on complex neuropsychiatric disease. *Neuron* **112**, 7–24 (2024).
2. Coe, B. P., Girirajan, S. & Eichler, E. E. The genetic variability and commonality of neurodevelopmental disease. *Am. J. Med. Genet. C Semin. Med. Genet.* **160C**, 118–129 (2012).
3. Huang, Y.-F. Unified inference of missense variant effects and gene constraints in the human genome. *PLoS Genet.* **16**, e1008922 (2020).
4. Bassett, D. S., Xia, C. H. & Satterthwaite, T. D. Understanding the Emergence of Neuropsychiatric Disorders With Network Neuroscience. *Biol. Psychiatry Cogn. Neurosci. Neuroimaging* **3**, 742–753 (2018).

5. Bray, N. J. & O'Donovan, M. C. The genetics of neuropsychiatric disorders. *Brain Neurosci. Adv.* **2**, 2398212818799271 (2019).
6. Pardiñas, A. F. *et al.* Common schizophrenia alleles are enriched in mutation-intolerant genes and in regions under strong background selection. *Nat. Genet.* **50**, 381–389 (2018).
7. Oishi, K. *et al.* Genetic risks of schizophrenia identified in a matched case-control study. *Eur. Arch. Psychiatry Clin. Neurosci.* **271**, 775–781 (2021).
8. Trubetskoy, V. *et al.* Mapping genomic loci implicates genes and synaptic biology in schizophrenia. *Nature* **604**, 502–508 (2022).
9. Sullivan, P. F. & Geschwind, D. H. Defining the Genetic, Genomic, Cellular, and Diagnostic Architectures of Psychiatric Disorders. *Cell* **177**, 162–183 (2019).
10. Visscher, P. M., Yengo, L., Cox, N. J. & Wray, N. R. Discovery and implications of polygenicity of common disease. *Science* **373**, 1468–1473 (2021).
11. Andreassen, O. A., Hindley, G. F. L., Frei, O. & Smeland, O. B. New insights from the last decade of research in psychiatric genetics: discoveries, challenges and clinical implications. *World Psychiatry Off. J. World Psychiatr. Assoc. WPA* **22**, 4–24 (2023).
12. Bourque, V.-R. *et al.* Genetic and phenotypic similarity across major psychiatric disorders: a systematic review and quantitative assessment. *Transl. Psychiatry* **14**, 171 (2024).
13. Gomez, A. M., Traunmüller, L. & Scheiffele, P. Neurexins: molecular codes for shaping neuronal synapses. *Nat. Rev. Neurosci.* **22**, 137–151 (2021).
14. Kim, H. Y., Um, J. W. & Ko, J. Proper synaptic adhesion signaling in the control of neural circuit architecture and brain function. *Prog. Neurobiol.* **200**, 101983 (2021).
15. Südhof, T. C. Synaptic Neurexin Complexes: A Molecular Code for the Logic of Neural Circuits. *Cell* **171**, 745–769 (2017).
16. Ushkaryov, Y. A., Petrenko, A. G., Geppert, M. & Südhof, T. C. Neurexins: synaptic cell surface proteins related to the alpha-latrotoxin receptor and laminin. *Science* **257**, 50–56 (1992).
17. Reissner, C., Runkel, F. & Missler, M. Neurexins. *Genome Biol.* **14**, 213 (2013).
18. Ullrich, B., Ushkaryov, Y. A. & Südhof, T. C. Cartography of neurexins: more than 1000 isoforms generated by alternative splicing and expressed in distinct subsets of neurons. *Neuron* **14**, 497–507 (1995).
19. Tabuchi, K. & Südhof, T. C. Structure and evolution of neurexin genes: insight into the mechanism of alternative splicing. *Genomics* **79**, 849–859 (2002).
20. Knight, D., Xie, W. & Boulianne, G. L. Neurexins and neuroligins: recent insights from invertebrates. *Mol. Neurobiol.* **44**, 426–440 (2011).
21. Kurshan, P. T. *et al.* γ-Neurexin and Frizzled Mediate Parallel Synapse Assembly Pathways Antagonized by Receptor Endocytosis. *Neuron* **100**, 150-166.e4 (2018).
22. Comoletti, D. *et al.* The macromolecular architecture of the extracellular domain of αNRXN1: domain organization, flexibility, and insights into trans-synaptic disposition. *Struct. Lond. Engl. 1993* **18**, 1044–1053 (2010).
23. Dean, C. *et al.* Neurexin mediates the assembly of presynaptic terminals. *Nat. Neurosci.* **6**, 708–716 (2003).
24. Scheiffele, P., Fan, J., Choih, J., Fetter, R. & Serafini, T. Neuroligin expressed in nonneuronal cells triggers presynaptic development in contacting axons. *Cell* **101**, 657–669 (2000).
25. Sons, M. S. *et al.* alpha-Neurexins are required for efficient transmitter release and synaptic homeostasis at the mouse neuromuscular junction. *Neuroscience* **138**, 433–446 (2006).

26. Zhang, C. *et al.* Neurexins physically and functionally interact with GABA(A) receptors. *Neuron* **66**, 403–416 (2010).
27. Missler, M. *et al.* Alpha-neurexins couple Ca2+ channels to synaptic vesicle exocytosis. *Nature* **423**, 939–948 (2003).
28. de Wit, J. & Ghosh, A. Specification of synaptic connectivity by cell surface interactions. *Nat. Rev. Neurosci.* **17**, 4–4 (2016).
29. Ullrich, B., Ushkaryov, Y. A. & Südhof, T. C. Cartography of neurexins: more than 1000 isoforms generated by alternative splicing and expressed in distinct subsets of neurons. *Neuron* **14**, 497–507 (1995).
30. Nguyen, T.-M. *et al.* An alternative splicing switch shapes neurexin repertoires in principal neurons versus interneurons in the mouse hippocampus. *eLife* **5**, e22757 (2016).
31. Treutlein, B., Gokce, O., Quake, S. R. & Südhof, T. C. Cartography of neurexin alternative splicing mapped by single-molecule long-read mRNA sequencing. *Proc. Natl. Acad. Sci. U. S. A.* **111**, E1291-1299 (2014).
32. Schreiner, D. *et al.* Targeted combinatorial alternative splicing generates brain region-specific repertoires of neurexins. *Neuron* **84**, 386–398 (2014).
33. Koehnke, J. *et al.* Splice form dependence of beta-neurexin/neuroligin binding interactions. *Neuron* **67**, 61–74 (2010).
34. Maury, E. A. *et al.* Schizophrenia-associated somatic copy-number variants from 12,834 cases reveal recurrent NRXN1 and ABCB11 disruptions. *Cell Genomics* **3**, 100356 (2023).
35. Fernando, M. B. *et al.* Phenotypic complexities of rare heterozygous neurexin-1 deletions. *Nature* **642**, 710–720 (2025).
36. Flaherty, E. *et al.* Neuronal impact of patient-specific aberrant NRXN1α splicing. *Nat. Genet.* **51**, 1679–1690 (2019).
37. Bastien, B. L., Cowen, M. H. & Hart, M. P. Distinct neurexin isoforms cooperate to initiate and maintain foraging activity. *Transl. Psychiatry* **13**, 367 (2023).
38. Brenner, S. The genetics of Caenorhabditis elegans. *Genetics* **77**, 71–94 (1974).
39. Churgin, M. A. *et al.* Longitudinal imaging of Caenorhabditis elegans in a microfabricated device reveals variation in behavioral decline during aging. *eLife* **6**, e26652 (2017).
40. Cowen, M. H. *et al.* Conserved autism-associated genes tune social feeding behavior in C. elegans. *Nat. Commun.* **15**, 9301 (2024).

Figures

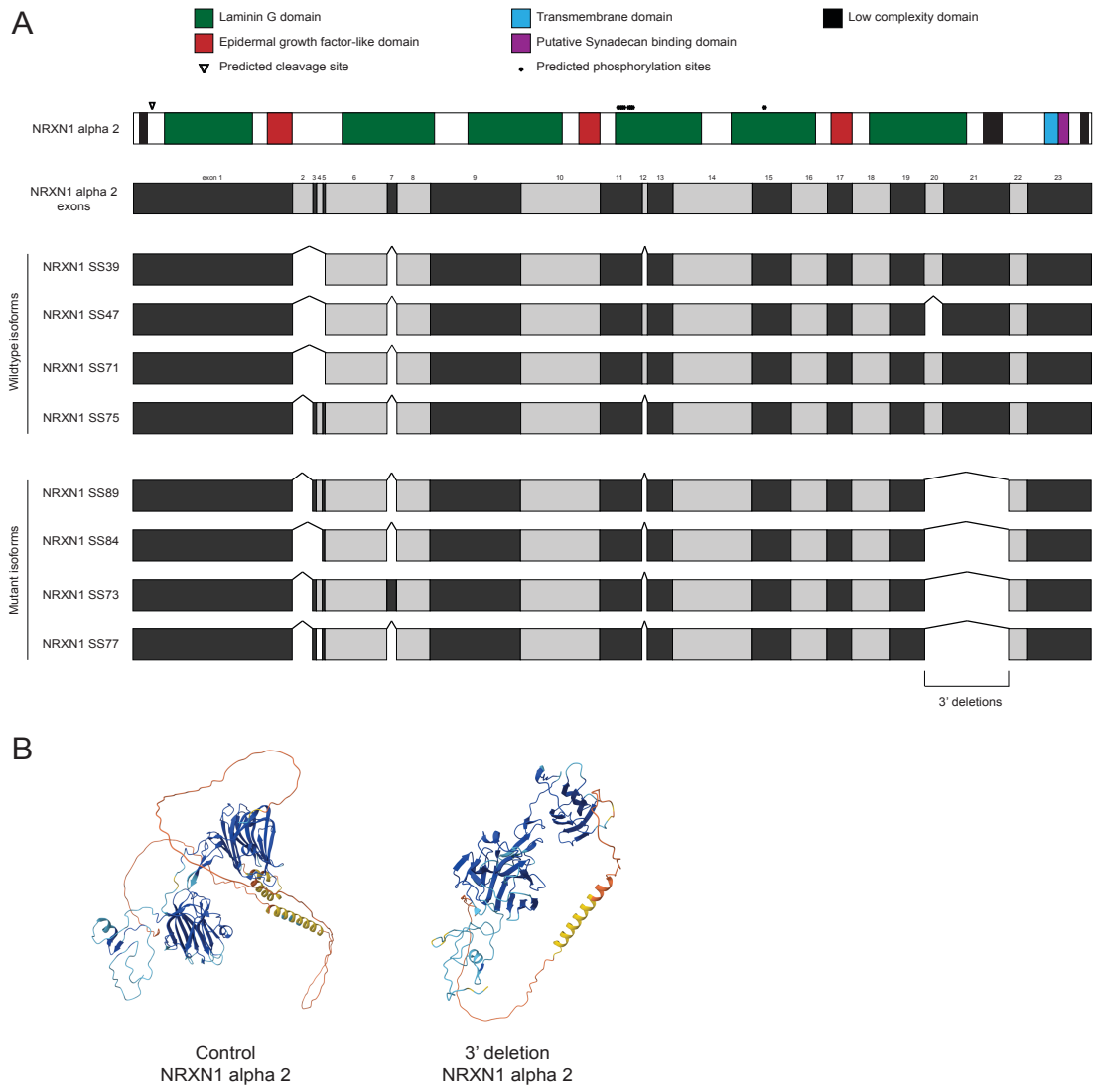

Figure 1. Schematic of control and 3' deletion NRXN1 isoforms. **(A)** Eight NRXN1 isoforms aligned against the genomic NRXN1 α2 (representing the longest alpha isoform), with known protein domain and architecture labelled. Control isoforms and splice differences are represented by interruptions within the CDS, while 3' NRXN1 deletion isoforms are separately labeled including splice differences and a shared deletion. (**B**) Alphafold models of exons 14-23 of control NRXN1 α2 isoform (left) and 3' deletion isoform SS84 (right).

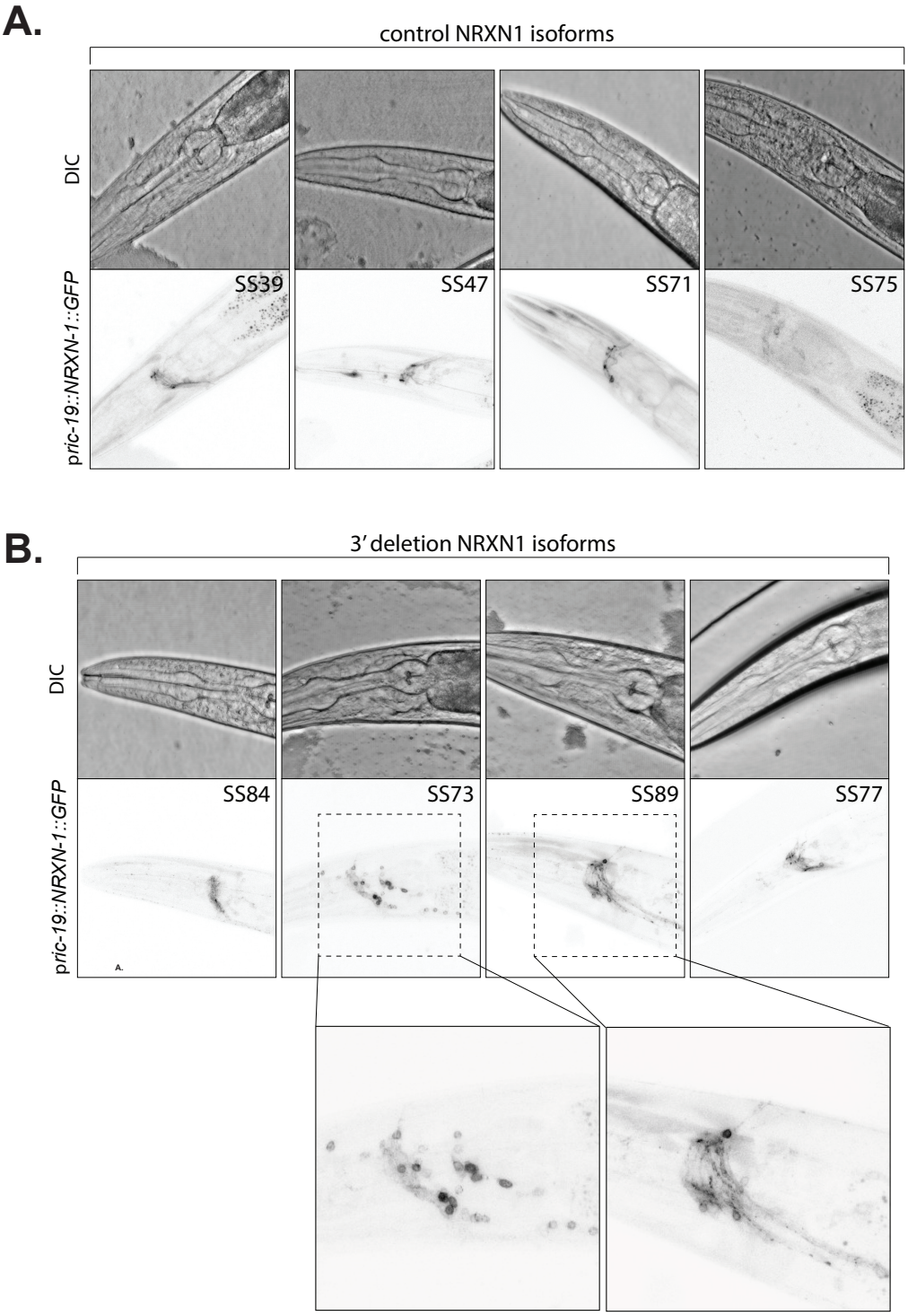

Figure 2. Expression and localization of NRXN1 isoforms in *C. elegans* neurons. (A) p*ric-19*::*gfp* was used to show expression of control NRXN1α isoforms (top panel), with the majority of the expression being localized to nerve ring surround the pharynx. The lower panel is DIC for

anatomical reference. **(B)** p*ric-19*::*gfp* was used to show expression of 3' deletion isoform variants of NRXN1α (top panel), with the majority of the expression being localized to nerve ring surround the pharynx. Insets show expression within cell bodies and head neurons, and abnormal punctate expression of NRXN1.

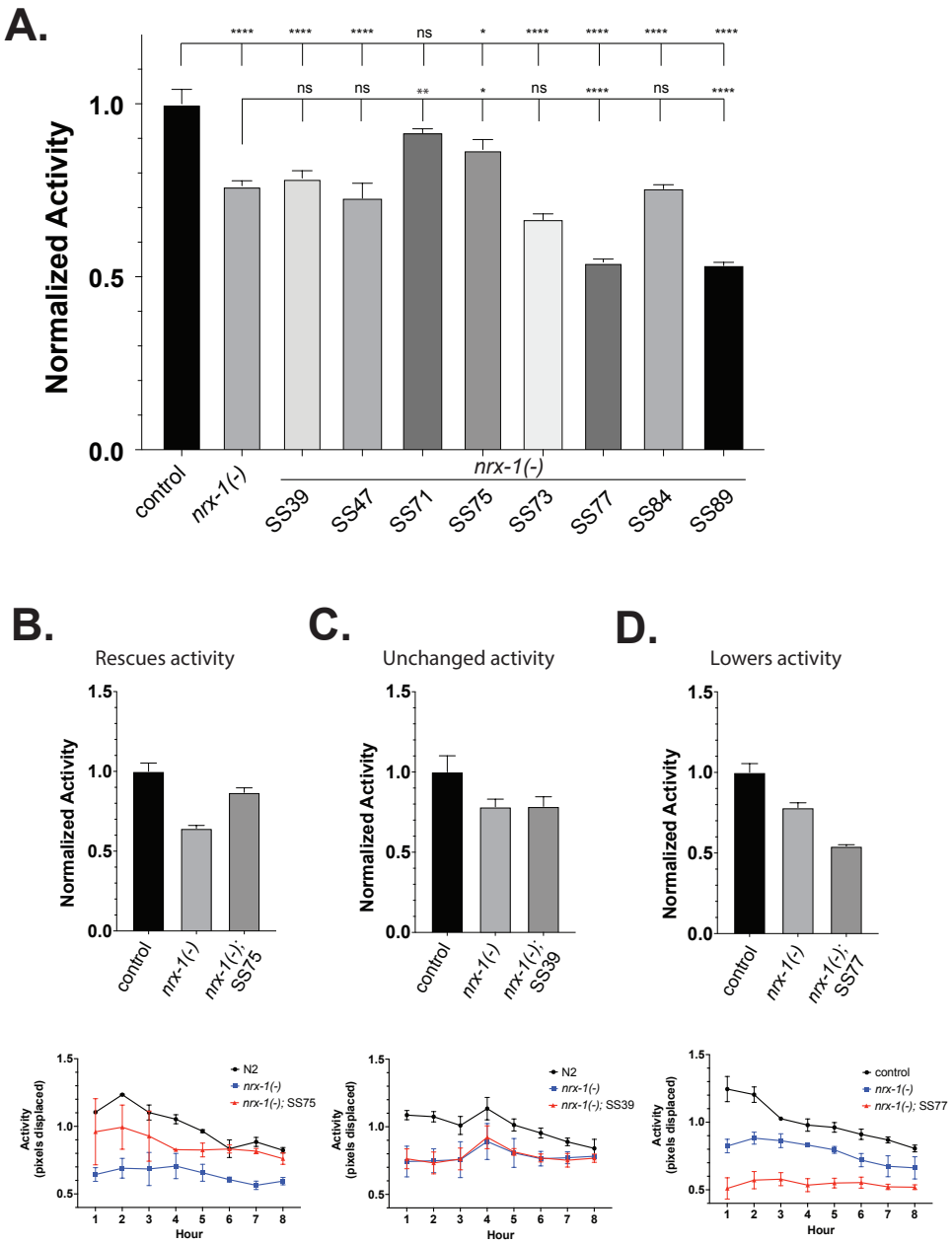

Figure 3. Comparison of NRXN1 isoforms on food-deprived activity levels. (A) Normalized activity values for animals without food. All *nrx-1(wy778)* and *NRXN1* animals were normalized within replicates to allow for pooling of replicates. A one-way ANOVA, with Tukey's post-hoc test was utilized to determine statistical significance. (B) SS75 is shown as an example of an

isoform variant that is able to partially rescue the *nrx-1(wyy78)* activity defect. Top panel shows normalized average across the full 8-hour time course. Bottom panel shows the 8-hour time series broken down by hour. **(C)** SS39 is shown as an example of an isoform variant whose activity is unchanged compared to the *nrx-1(wyy78)*. Top panel shows normalized average across the full 8-hour time course. Bottom panel shows the 8-hour time series broken down by hour. **(D)** SS77 is shown as an example of an isoform variant whose activity is significantly worse compared to the *nrx-1(wyy78)*, thus representing a gain of function phenotype. Top panel shows normalized average across the full 8-hour time course. Bottom panel shows the 8-hour time series broken down by hour.

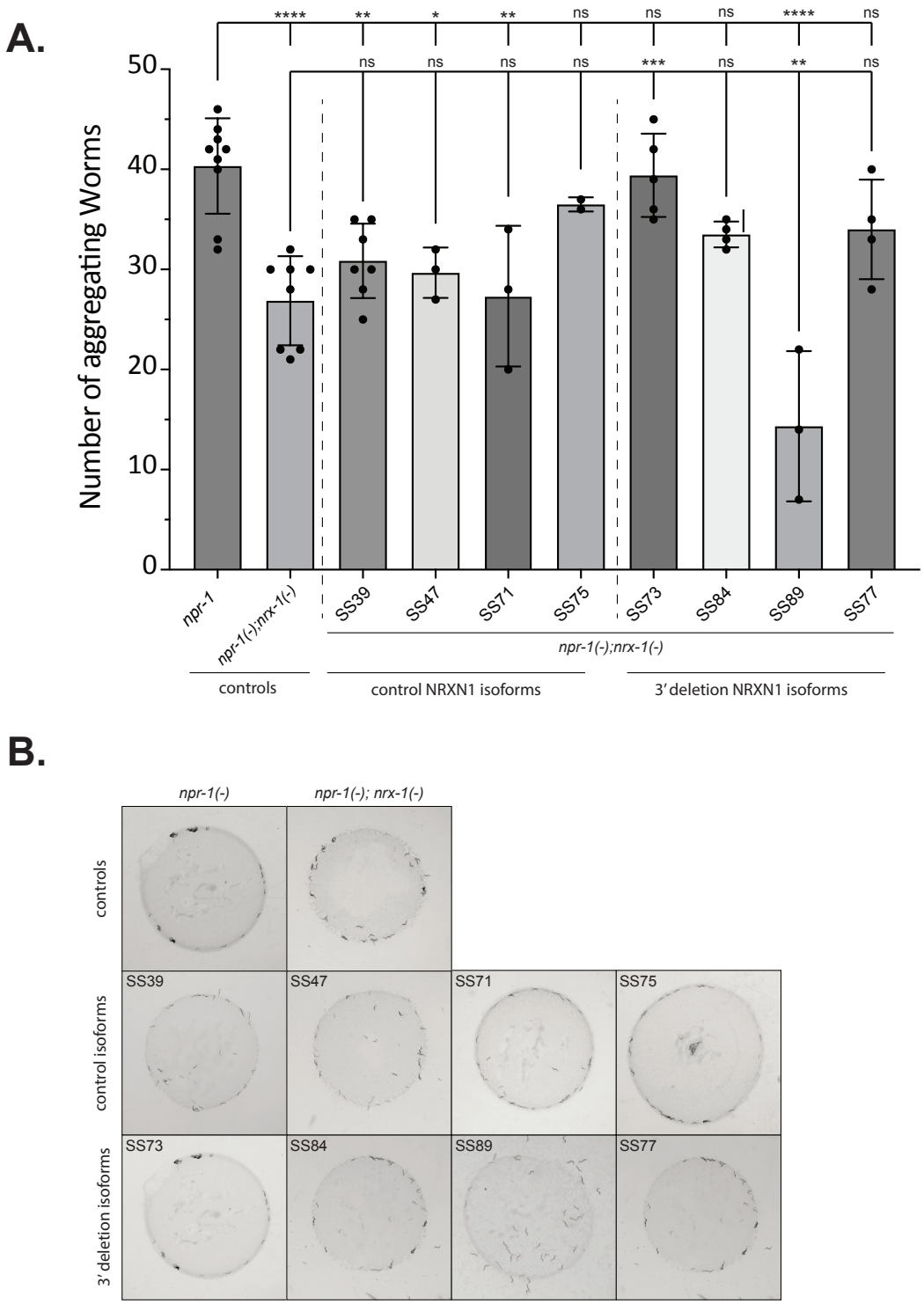

Figure 4. NRXN1 isoforms differentially impact social feeding behavior. (A) In comparison to *npr-1(ad609)* controls with high aggregation, *npr-1(ad609);nrx-1(wy778)* controls have significantly reduced levels of aggregation. Control NRXN1 isoforms are shown in the left panel, while 3' deletion isoform variants are shown on the right. Bar graphs represent the mean values

across biological replicates (each replicate indicated by a dot). Error bars show stand error of mean. One-way ANOVA with Tukey's post-hoc test was used for statistical comparisons, with p-values indicated in standard format (p=0.05(*), p=0.01(**), p=0.001(***), p= <0.001 (****)). **(B)** Representative images of aggregation behavior.

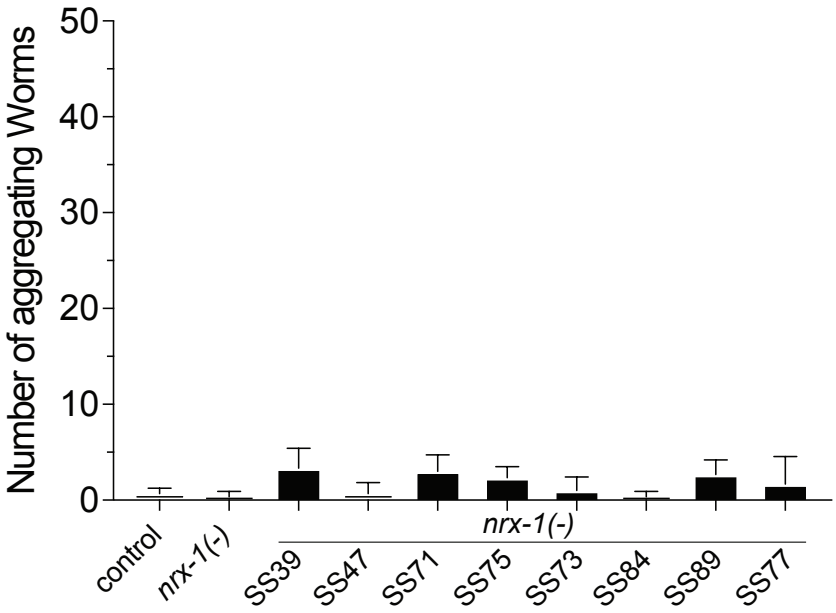

Supplemental Figure 1. Expression of NRXN1 isoforms does not induce aggregation behavior. In addition to control (N2 Bristol) and *nrx-1(wy778)*, 8 NRXN1 isoforms (4 control isoforms and 4 3' deletion isoforms) were tested for aggregation behavior in the solitary feeding N2 Bristol strain background with and without *nrx-1(wy778)* (as opposed to the social feeding and aggregating *npr-1(ad609)* background).